Control of Wheeled Robots Using GNSS and Inertial Navigation: Control Law Synthesis and Experimental Results

Conference Paper · September 2006

CITATIONS
8

READS
164

6 authors, including:

Lev Rapoport
Institute of Control Sciences
75 PUBLICATIONS **422** CITATIONS

SEE PROFILE

A. V. Pesterev
Russian Academy of Sciences
59 PUBLICATIONS **566** CITATIONS

SEE PROFILE

Control of Wheeled Robots Using GNSS and Inertial Navigation: Control Law Synthesis and Experimental Results

L. Rapoport, M. Gribkov, A. Khvalkov, I. Matrosov, A. Pesterev, M. Tkachenko, *Javad GNSS*

BIOGRAPHY

Lev B. Rapoport received an MSEE degree from the radiotechnical department of the Ural Polytechnic Institute, Sverdlovsk, in 1976, a PhD degree in Automatic Control from the Institute of System Analysis, Moscow, in 1982, and a DrSc degree in Automatic Control from the Institute of Control Sciences, Moscow, in 1995, where he serves as a head of the non-linear systems control laboratory. Since 1994 till 1998 he worked for Ashtech. Since 1998 was with Javad Positioning Systems, since 2001 till 2005 he was with Topcon Positioning Systems and Javad Navigation Systems. Currently he is with Javad GNSS.

Mikhail A. Gribkov received an MSCS degree from the cybernetics department of the Moscow Engineering and Physics Institute in 2003. Since 2004 till 2005 he was with Topcon Positioning systems. Currently he is with Javad JNSS and works on computer vision in the RTK and Machine Control team.

Alexander A. Khvalkov received an MSEE degree from the radiotechnical department of the Moscow Aviation Institute in 1991. Since 1997 was with Javad Positioning Systems, since 2001 was with Topcon Positioning Systems and Javad Navigation Systems. Currently he is with Javad GNSS where he is engaged in RTK and INS firmware design in the RTK and Machine Control team.

Ivan V. Matrosov received an MS degree in mathematics from the mechanical-mathematical department of the Lomonosov Moscow State University in 1996, a PhD degree in Differential Equations from the same university in 2001. Since 2001 he was with Topcon Positioning Systems and Javad Navigation Systems. Currently he is with Javad GNSS, RTK and Machine Control team.

Alexander V. Pesterev received an MS degree in applied mathematics from the Moscow Institute of Physics and Technology in 1976 and a PhD degree in Automatic Control from the Institute for System Analysis, Moscow, in 1990. Since 1997, he has been working as a senior researcher at the Institute for System Analysis of Russian Academy of Sciences. In 2004, he joined Topcon Positioning Systems, and, since 2005, he is with Javad GNSS in the RTK and Machine Control group.

Michael Ya. Tkachenko received an MS degree in mechanics from the mechanical-mathematical department of the Lomonosov Moscow State University in 1987. Since 1993 till 2003 he worked for Ashtech. Since 2003 till 2005 he worked for Topcon Positioning Systems. Currently he is with Javad GNSS in the RTK and Machine Control group.

ABSTRACT

The paper addresses the problem of automatic steering of the wheeled robot like a car to drive it through desired path stored in the controller memory. More specifically, a target point selected on the body of the robot must follow the target path. The target point must be driven to the target path from the arbitrary position and arbitrary orientation of the robot platform and its motion along the target path must be stabilized. The GNSS receiver and inertial sensors are used to measure the position, velocity, and orientation. The orientation of the body of the robot is necessary to translate position of the receiver antenna to the position of the target point. Orientation angles are also used in the synthesis of the control law.

The problem setup described above is not new. An extensive literature is devoted to it (see [1]–[4] and references cited there). The control law synthesis is described in [3,4], but two-sided constraints on the front wheels angle are not taken into account accurately. On the other side, these constraints affect badly the stability of the motion of the robot and degrade quality of the automatic control. The properties of the transient processes happen to be dependent on the initial position and initial orientation of the robot. For some initial data the lateral displacement of the target point from the target trajectory decreases in the exponential manner predicted

during the control law synthesis, while for another initial data the transient process of the lateral displacement behaves very oscillatory.

The problem of estimation of the attraction domain in the 'position – orientation' space that guarantees given exponential rate of decrease of the lateral displacement is addressed in the paper. The modern techniques based on absolute stability theory and linear matrix inequalities (LMI) [5, 6] is used.

The paper also includes description of the Kalman filtering scheme that integrates GNSS and inertial data for the single antenna case.

INTRODUCTION

The problem of the control of a wheeled mobile robot is considered in the paper. The system consists of a single dual-band GPS/GLONASS receiver and the INS block mounted on a vehicle. The single-antenna architecture significantly restricts the ability of the GNSS component to observe the attitude. Moreover, to observe two angles – pitch and heading – using the GNSS velocity vector, the system is supposed to satisfy an additional nonholonomic constraint. In terms of the dynamics of wheeled mobile robots, like cars or tractors, a nonholonomic constraint means motion without lateral slipping. Even in the presence of this constraint, the third angle – roll – is still not observable from only the GNSS data. Integration with the inertial data is used to estimate the complete attitude. To calibrate the roll bias, a special procedure must be performed, whereas the pitch and heading biases are estimated in real time as components of the state vector of the Kalman filter.

Figure 1 below shows a schematic of the wheeled robot. For the sake of brevity, in the description of the control law, we restrict ourselves to the planar case. However, the three-dimensional case will be addressed when describing the GNSS/INS integration scheme. The following notation is used:

- X is the target point (the midpoint of the rear axis),
- V is the linear velocity of the target point $v = \|V\|$,
- u is the current curvature of the trajectory of the target point,
- X_0 is the current curvature center,
- α_1 and α_2 are angles of the front wheels, and
- L, H are linear dimensions of the platform.

The control goal is to force the target point to follow a target path, denoted by the solid green line in Fig. 1, while the dashed green line denotes an actual trajectory of the target point. The control is applied to the front wheels. The path is approximated by segments of constant or variable curvature, such as straight lines, segments of circles, or splines. The path data required for the approximation are collected in the course of the first (manual) drive along the desired path. After the first run, the target path is stored in the memory, and the system is capable of repeating it. The vehicle approaches the desired path starting from an arbitrary initial position and orientation (see Fig. 1). The following relationships take place:

$$\frac{uL}{1-uH/2} = tg\alpha_1, \quad \frac{uL}{1+uH/2} = tg\alpha_2. \qquad (1)$$

Equations (1) establish relationships between the current curvature u and the front wheels angles α_1 and α_2. Relationships (1) make it possible to simplify the dynamic model of the robot and consider u as a control variable:

$$\begin{aligned} \dot{x} &= v\cos\theta, \\ \dot{y} &= v\sin\theta, \\ \dot{\theta} &= vu. \end{aligned} \qquad (2)$$

Constraints on the wheels angles impose the two-sided constraints on the control

$$-\bar{u} \le u \le \bar{u}\,. \qquad (3)$$

System (2) subject to constraints (3) can be represented as

$$\begin{aligned} \dot{x} &= v\cos\theta, \\ \dot{y} &= v\sin\theta, \\ \dot{\theta} &= v\,\mathrm{sat}_{\bar{u}}(u), \end{aligned} \qquad (4)$$

where $\mathrm{sat}_{\bar{u}}(u)$ stands for the 'saturation' operator.

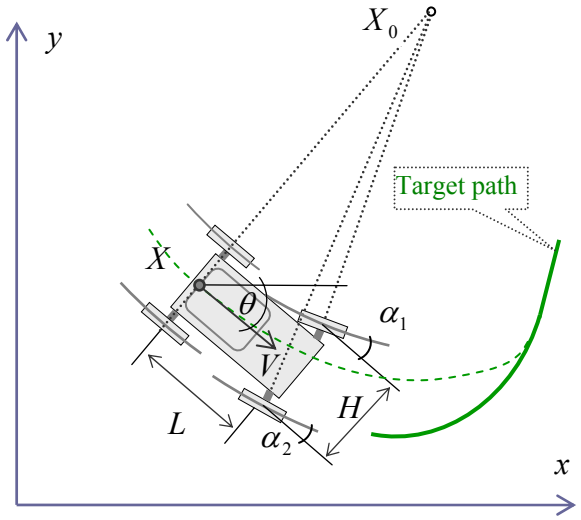

Fig. 1. Schematic description of the robot.

In this paper, the control law is constructed using the feedback linearization approach [7]. If this control law is applied to system (2), the resulting feedback system turns to a linear system. This control law is then applied to system (4) which is of primary interest to us. The resulting feedback system is not linear now, because of the 'saturation' operator. The behavior of this nonlinear system is not a priori clear, and stability analysis of the closed-loop system is required. It is performed by using

quadratic Lyapunov functions. Ellipsoidal estimation of the attraction domain that guarantees exponential stability of the closed-loop system is made using techniques of absolute stability and LMI's [5, 6].

To implement automatic control in the real world conditions, the position and velocity of the target point must be available for either measurement or at least estimation. In the present work, these quantities are estimated in the real time using the GNSS/INS integrated system as mentioned above. The antenna is located on the roof, the INS block is firmly attached to the body of the robot. The position and velocity of the target point is estimated during the combined filtering of all measurements. The orientation of the body is necessary to translate position and velocity of the receiver antenna to the position and velocity of the target point. The orientation is also used in the control law synthesis. The smoothed position and velocity is estimated at up to 100 Hz rate.

The following problems and results are discussed in the paper:

1. Synthesis of a control algorithm for steering front wheels.
2. Influence of the two-sided constraints on the control quality.
3. Influence of the internal dynamics of the actuators on the vehicle behavior.
4. Numerical scheme of filtering.
5. Initial calibration and biases stability.
6. Testing results on the car model.

CONTROL LAW SYNTHESIS

For the sake of brevity, we assume that the target trajectory is the straight line $y = 0$. Let us also assume that the linear velocity is bounded,

$$0 < v_0 \le v(t) \le v_1 \qquad (5)$$

and the orientation angle satisfies the constraint

$$\cos\theta(t) \ge \varepsilon > 0. \qquad (6)$$

The last constraint will be further removed. Let us change variables (as it was done in [4]): $z_0 = x$, $z_1 = y$, $z_2 = tg\theta$. Let $'$ denote differentiation with respect to the variable x. Then, system (4) takes the form

$$\begin{aligned} z_0' &= 1, \\ z_1' &= z_2, \\ z_2' &= \mathrm{sat}_{\bar{u}}(u)(1+z_2^2)^{\frac{3}{2}}. \end{aligned} \qquad (7)$$

Let $\lambda > 0$, and let us select the control law as

$$u = -\frac{\lambda^2 z_1 + 2\lambda z_2}{(1+z_2^2)^{\frac{3}{2}}}. \qquad (8)$$

Removing temporarily constraint (3) (or setting $\bar{u} = \infty$, or ignoring the $\mathrm{sat}_{\bar{u}}(u)$ operator) and substituting (8) into (7), we obtain

$$z_1'' + 2\lambda z_1' + \lambda^2 z_1 = 0. \qquad (9)$$

This differential equation means exponential rate of decrease of variables z_1 and z_2 with an exponent $-\lambda$. However, control (8) does not satisfy constraints (3). On the other hand, system (7),(8), which can be rewritten as

$$\begin{aligned} z_1' &= z_2, \\ z_2' &= -\mathrm{sat}_{\bar{u}}\left(\frac{\lambda^2 z_1 + 2\lambda z_2}{(1+z_2^2)^{\frac{3}{2}}}\right)(1+z_2^2)^{\frac{3}{2}} \end{aligned} \qquad (10)$$

(the trivial equation $z_0' = 1$ is omitted), does not provide exponential rate of decrease of variables. The picture below shows plots of z_1 obtained by solving system (9) ($\bar{u} = \infty$, solid green line) and (10) ($\bar{u} = 0.1$, dashed red line) with the initial data $z_1 = 1$, $z_2 = -1$.

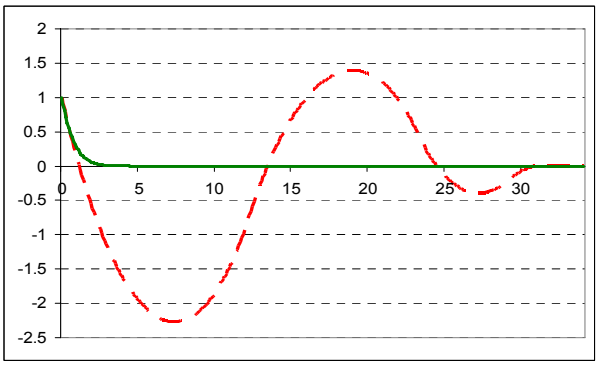

Fig. 2. Plots of the lateral distance to the target trajectory without (solid green line) and with (dashed red line) constraints on the control

Moreover, behavior of the nonlinear system (1) significantly depends on the initial data. The picture below illustrates this.

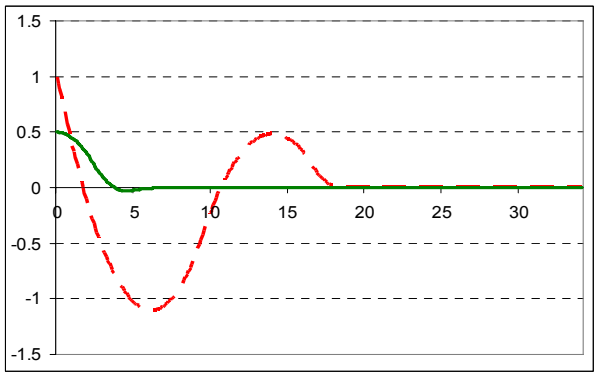

Fig. 3. Plots of the lateral distance to the target trajectory for the system (10) with different initial data.

The solid green line in Fig. 3 corresponds to the initial data $z_1 = 0.5$, $z_2 = 0$, while the dashed red line corresponds to the initial data $z_1 = 1$, $z_2 = -0.6$. Inappropriate choice of the initial position and orientation leads to the overshot in the automatic control. Two pictures below illustrate unsuccessful behavior of the robot. The goal was to follow the centerline of the concrete lane. Being started from improper orientation (Fig. 4a) the robot was not able to fit into the limited width of the path (Fig. 4b).

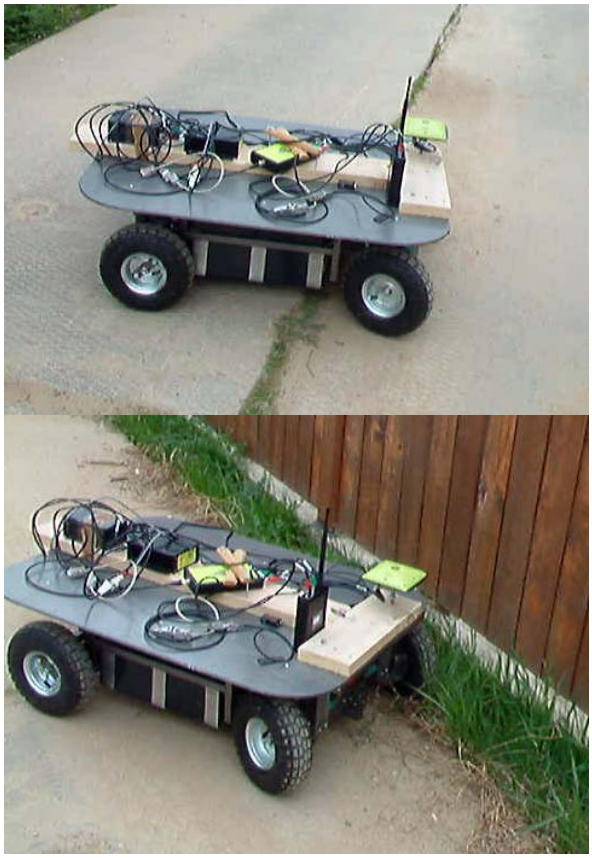

Fig. 4. Initial position (a) and overshot (b) in the middle of trajectory.

Thus, we arrive at the problem of estimation of the attraction domain of desired size that guarantees a specified exponential rate of convergence (the attraction domain belongs to the circle of a specified radius). The radius of the circle may be chosen as a width of the lane, see Fig. 4b.

ESTIMATION OF THE ATTRACTION DOMAIN

Let us denote $z = (z_1, z_2)^T$, where ^{T} denotes matrix transposition. Let us introduce a quadratic Lyapunov function,

$$V(z) = z^T P z, \qquad (11)$$

where $P > 0$ is a symmetric positive definite matrix. Moreover, we impose an additional constraint on it:

$$P \geq I, \qquad (12)$$

where I is the identity matrix; the notation $A \geq B$ means that $A - B \geq 0$. Introduce the notation $\frac{d(V(z))}{dx}$ for the total derivative of the Lyapunov function with respect to system (10). Let μ be a positive constant satisfying the inequality $\mu \leq \lambda < 0$, and let

$$\frac{d(V(z))}{dx} + 2\mu V(z) \leq 0. \qquad (13)$$

From (13), it follows that the Lyapunov function decreases exponentially with the exponent -2μ. We say that the vector function $z(x)$ decreases exponentially with the exponent $-\mu$ if there exists a Lyapunov function (11) satisfying (13). We will seek an estimate for the attraction domain in the form

$$\Omega(\alpha) = \left\{ z \in R^2 : V(z) \leq \alpha^2 \right\} \qquad (14)$$

where $V(z)$ satisfies (13) for $z \in \Omega(\alpha)$. In view of (12), region (14) belongs to the circle of radius α (Fig. 5a). If, in addition to (14), the condition $\sigma_{\min}(P) = 1$ holds, where $\sigma_{\min}(P)$ is the minimal eigenvalue of the matrix P, this region belongs to the circle and is tangent to it (Fig. 5b).

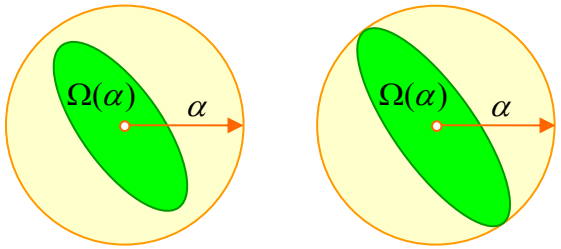

Fig. 5 (a) $P \geq I$, (b) $P \geq I$ and $\sigma_{\min}(P) = 1$

Along with system (10), consider the linear nonstationary system

$$\begin{aligned} z_1' &= z_2, \\ z_2' &= -\beta(x)(\lambda^2 z_1 + 2\lambda z_2), \end{aligned} \qquad (15)$$

where $\beta(x) \in [0,1]$. The following statement is proven in [8]: if $z \in \Omega(\alpha)$, then

$$k\sigma \leq \mathrm{sat}_{\bar{u}}\left(\frac{\sigma}{(1+z_2^2)^{\frac{3}{2}}} \right)(1+z_2^2)^{\frac{3}{2}} \leq \sigma, \qquad (16)$$

$$-\sigma_0 \leq \sigma \leq \sigma_0, \qquad (17)$$

where

- $\sigma = \lambda^2 z_1 + 2\lambda z_2$,
- $k = \min\left\{\frac{\bar{u}}{\sigma_0}, 1\right\}$,
- $\sigma_0 = \sqrt{c^T P^{-1} c}$,
- $c = (\lambda^2, 2\lambda)^T$.

Due to (16), if the whole trajectory $z(x)$ of the system belongs to the domain $\Omega(\alpha)$, then $z(x)$ satisfies also system (15) for some function $\beta(x) \in [k,1]$. If every solution of system (15) with the initial point belonging to the domain $\Omega(\alpha)$ remains in the domain and condition (13) holds along the trajectory, then every trajectory of system (10) starting in $\Omega(\alpha)$ also remains there and condition (13) holds along the trajectory. Let us denote

$$A_\beta = \begin{pmatrix} 0 & 1 \\ -\beta\lambda^2 & -2\beta\lambda \end{pmatrix}.$$

Summing up statements given above, we arrive at the following

Theorem. Suppose that, for some $\alpha > 0$, $0 < \mu \le \lambda$, and $0 < \beta \le 1$, there exist a solution P to the linear matrix inequalities

$$PA_1 + A_1^T P + 2\mu P \le 0, \quad (18)$$

$$PA_\beta + A_\beta^T P + 2\mu P \le 0, \quad (19)$$

$$\begin{bmatrix} P & c \\ c^T & \frac{\bar{u}^2}{\alpha^2\beta^2} \end{bmatrix} \ge 0, \quad (20)$$

$$P \ge I. \quad (21)$$

Then, the set $\Omega(\alpha)$ is an attraction domain for system (10), and every trajectory starting in $\Omega(\alpha)$ remains there and has an exponential rate of decrease with the exponent $-\mu$.

Numerical methods for testing LMIs for feasibility are described, for example, in [6]. These methods reduce the problem to a convex optimization problem. There are many packages for solving LMIs. In our numerical experiments, we used 'LMI Lab' toolbox included in Matlab 7.

To illustrate the method, we used the following parameters: $\bar{u} = 0.1$ and $\lambda = 2$. Figure 6 shows two ellipsoidal domains. The bigger ellipsoid corresponds to the values $\mu = 0.01$ and $\alpha = 0.245$, and the smaller one, to $\mu = 1.6$ and $\alpha = 0.08$. The blue lines show trajectories of system (10).

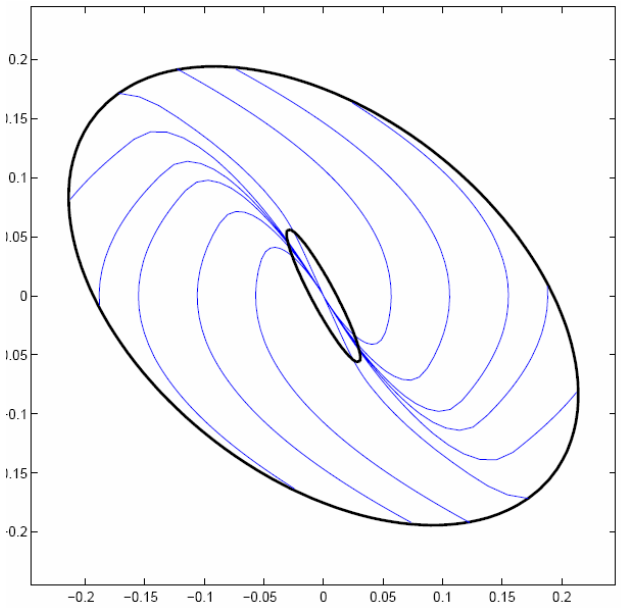

Fig. 6. Attraction domains and trajectories of the system.

INTEGRATION OF GNSS AND INERTIAL NAVIGATION SENSORS

To calculate the control as described above, one needs the planar position of the target point and the orientation angle. The target point is located in the middle of the rear axis and cannot be measured directly. Obviously, the GNSS antenna is located on the roof of the vehicle. Moreover, to estimate the 2D position of the target point using 3D position of the antenna located on the roof, one needs 3D orientation of the body. The GNSS receiver is augmented by an IMU block to produce the smoothed position of the target point, velocity of the target point, and orientation. This section contains description of the integrated system used in our experiments.

The system consists of a single dual-band dual-system GPS/GLONASS receiver and the IMU unit (see [9]). Both units are firmly attached to the vehicle body. We restrict our consideration to wheeled vehicles, like cars or tractors. The key feature of such vehicles is that every wheel moves without cross-track slippage. This is the so-called nonholonomic kinematic constraint.

From now on, the position vectors are supposed to be three-dimensional. Let us introduce the following notation:

- $X = (x, y, z)^T$ is the target point in the WGS-84 frame;
- X_{GNSS} is the receiver's antenna position in the WGS-84;
- $\vec{n}$, $\vec{r}$, $\vec{d}$ are the 'nose', 'right', and 'down' body frame vectors, respectively;

- v is the scalar velocity of the target point X;

- $C_{IMU-WGS84} = C_{LOC-WGS84} C_{IMU-LOC}$ is the orthogonal transformation matrix from the vehicle body frame to the WGS-84 frame; it is supposed that the IMU frame is aligned with the body frame;

- $\omega^{\times} = \begin{pmatrix} 0 & -\omega_3 & \omega_2 \\ \omega_3 & 0 & -\omega_1 \\ -\omega_2 & \omega_1 & 0 \end{pmatrix}$ is the skew-symmetric matrix composed of the vector $\omega = (\omega_1, \omega_2, \omega_3)'$;

- ω_{IMU} is the angular velocity vector measured in the body frame (gyro measurements vector);

- a_{IMU} is the acceleration vector measured in the body frame (accelerometer measurements vector);

- ω_{earth} is the vector of the Earth angular velocity measured in the WGS-84 frame;

- r_{IMU} is the shift vector between the body frame origin and the point where the IMU sensors are attached (all sensors are supposed to be centered at one point) measured in the body frame;

- r_{GNSS} is the shift vector between the body frame origin and the attachment point of the GNSS antenna (all sensors are supposed to be centered at one point) measured in the body frame;

- X_{IMU} is the IMU position in the WGS-84 frame;

- g is the local gravity vector.

Taking into account the nonholonomic constraint, we have the following equation for the velocity of the target point expressed in the WGS-84

$$\dot{X} = v C_{IMU-WGS84} i_n, \tag{22}$$

where $i_n = (1,0,0)'$. In terms of the notation defined above, the Poisson equation takes the form

$$\dot{C}_{IMU-WGS84} = C_{IMU-WGS84} \omega_{IMU}^{\times} - \omega_{earth}^{\times} C_{IMU-WGS84}. \tag{23}$$

Further, $X_{IMU} = X + C_{IMU-WGS84} r_{IMU}$. Applying the Coriolis theorem to this equation, we obtain

$$\begin{aligned} \dot{v} i_n &= a_{IMU} + C_{IMU-WGS84}^T (C_{LOC-WGS84} g \\ &- \omega_{earth}^{\times} \omega_{earth}^{\times} X - v \omega_{earth}^{\times} C_{IMU-WGS84} i_n) \\ &- v \omega_{IMU}^{\times} i_n - \dot{\omega}_{IMU}^{\times} r_{IMU} - \omega_{IMU}^{\times} \omega_{IMU}^{\times} r_{IMU}. \end{aligned} \tag{24}$$

Multiplying (24) by i_n^T and denoting the right-hand side of the equation obtained as $f(X, v, C_{IMU-WGS84}, a_{IMU}, \omega_{IMU}^{\times}, \dot{\omega}_{IMU}^{\times}, r_{IMU})$, we get the kinematic equations

$$\begin{pmatrix} \dot{x} \\ \dot{v} \\ \dot{C}_{IMU-WGS84} \end{pmatrix} = \begin{pmatrix} v C_{IMU-WGS84} i_n \\ f(X, v, C_{IMU-WGS84}, a_{IMU}, \omega_{IMU}^{\times}, \dot{\omega}_{IMU}^{\times}, r_{IMU}) \\ C_{IMU-WGS84} \omega_{IMU}^{\times} - \omega_{earth}^{\times} C_{IMU-WGS84} \end{pmatrix} \tag{25}$$

Further,

$$X_{GNSS} = X + C_{IMU-WGS84} r_{GNSS}, \tag{26}$$

$$\begin{aligned} \dot{X}_{GNSS} &= v C_{IMU-WGS84} i_n \\ &+ (C_{IMU-WGS84} \omega_{IMU}^{\times} - \omega_{earth}^{\times} C_{IMU-WGS84}) r_{GNSS} \end{aligned}. \tag{27}$$

Linearizing the set of equations (25) in the neighborhood of the reference trajectory, we obtain the following set of equations in errors:

$$\begin{pmatrix} \delta\dot{x} \\ \delta\dot{v} \\ \delta\dot{\omega}_C \\ \delta\dot{\omega}_{IMU} \\ \delta\dot{a}_n \end{pmatrix} = \left(\begin{array}{c|c|c|c|c} 0 & C_{IMU-WGS84} i_n & -v C_{IMU-WGS84} i_n^{\times} & 0 & 0 \\ \hline 0 & 0 & F_0 & F_1 & 1 \\ \hline 0 & 0 & -\omega_{IMU}^{\times} & I & 0 \\ \hline 0 & 0 & 0 & 0 & 0 \\ \hline 0 & 0 & 0 & 0 & 0 \end{array}\right) \times \begin{pmatrix} \delta x \\ \delta v \\ \delta\omega_C \\ \delta\omega_{IMU} \\ \delta a_n \end{pmatrix} + \begin{pmatrix} 0 \\ 0 \\ 0 \\ \xi_\omega \\ \xi_a \end{pmatrix}, \tag{28}$$

where

- δx is the correction to the position;

- δv is the correction to the linear velocity;

- $\delta\omega_C$ is the correction vector to the rotation matrix $C_{IMU-WGS84} \to C_{IMU-WGS84}(I + \delta\omega_C^{\times})$;

- $\delta\omega_{IMU}$ is the additive gyro bias modeled as a random walk;

- δa_n is the additive 'nose' accelerometer bias modeled as a random walk;

- $F_0 = i_n^T [C_{IMU-WHS84}^T (C_{LOC-WGS84} g - \omega_{earth}^{\times} \omega_{earth}^{\times} X - v \omega_{earth}^{\times} C_{IMU-WGS84} i_n)]^{\times}$;

- $F_1 = i_n^T [(\omega_{IMU}^{\times} r_{IMU})^{\times} + \omega_{IMU}^{\times} r_{IMU}^{\times}]$;

- ξ_ω and ξ_a are appropriate generating white noise vectors.

To derive the Kalman filtering scheme, we need to complete the errors model by the set of observation equations, which are derived by linearizing equations (26) and (27):

$$\begin{aligned}
&\delta x - C_{IMU-WGS84} r^{\times}_{GNSS} \delta\omega_C \\
&= X_{GNSS} - X - C_{IMU-WGS84} r_{GNSS} + \varepsilon_X \\
&C_{IMU-WGS84}[\delta v i_n - (v i_n + \omega^{\times}_{IMU} r_{GNSS})^{\times} \delta\omega_C \\
&- r^{\times}_{GNSS} \delta\omega_{IMU}] \\
&= \dot{X}_{GNSS} - v C_{IMU-WGS84} i_n \\
&- (C_{IMU-WGS84} \omega^{\times}_{IMU} - \omega^{\times}_{earth} C_{IMU-WGS84}) r_{GNSS} + \varepsilon_V
\end{aligned} \tag{29}$$

where ε_X and ε_V are appropriate measurement white noise vectors.

EXPERIMENTAL RESULTS

Experimental results were obtained with an electric car shown in Fig. 7. It is equipped with the set of equipment listed in the previous section. The control algorithm is embedded into firmware if the IMU block.
The receiver works in the carrier phase differential (RTK) mode using the UHF modem (see Fig. 7) for the data link.

Fig. 7. The model of the wheeled robot.

A typical plot of the lateral error is shown in Fig. 8. The result was obtained when moving along a straight line in the settled steady mode. The maximum value of the error in the settled mode does not exceed 0.02 m.

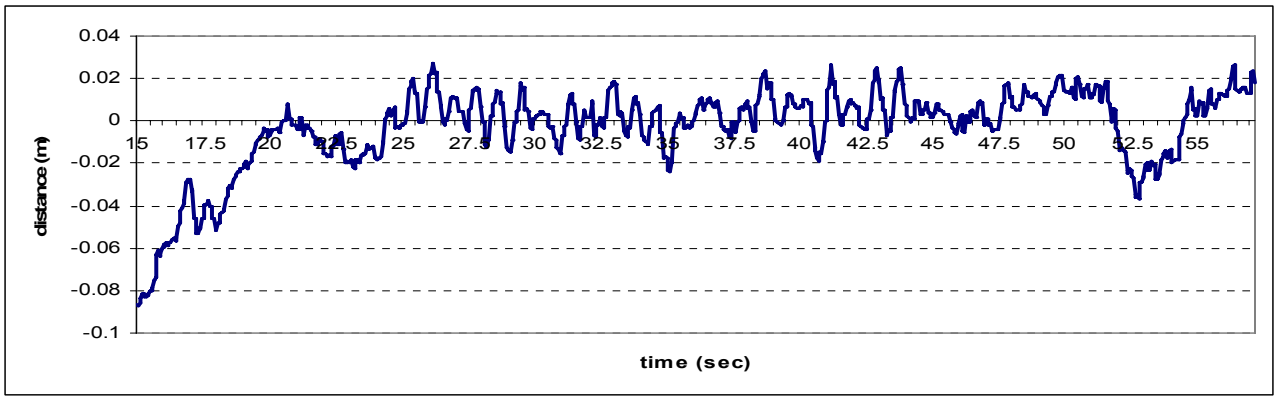

Fig. 8. Plot of the lateral displacement of the target point from the target trajectory.

EXTENSIONS AND FUTURE WORK

That was supposed that the front wheels actuators respond immediately in equations (2) and (4). Actually, of course the instant value of the current curvature u is subject to certain differential equation describing internal dynamics of the front wheels actuators. The method of the attraction domain estimation described above can be extended to the case of the actuators dynamic. That will lead to the greater number of linear matrix inequalities and larger dimensions of the matrix P, but generally the method of estimation is the same.

Integration with the computer vision may be considered as a future work, where the computer vision will be used for better estimation of linear and angular velocities.

REFERENCES

[1] C. Samson. Control of Chained Systems: Application to Path Following and Time-Varying Point-Stabilization of Mobile Robots // IEEE Trans. Automat. Contr. 1995. **v** 40. No. 1. p. 64-77.

[2] I. Kolmanovsky, N.H. McClamroch. Developments in Nonholonomic Control Problems // IEEE Control Syst. 1995. No. 12. p. 20-36.

[3] B. Thuilot, C. Cariou, P. Martinet, M. Berducat. Automatic Guidance of a Farm Tractor Relying on a Single CP-DGPS // Autonomous Robots. 2002. No. 13. p. 53-61.

[4] L. Cordesses, C. Cariou, M. Berducat. Combine Harvester Control Using Real Time Kinematic GPS // Precision Agriculture. 2000. No. 2. p. 147-161.

[5] L.B. Rapoport. Estimation of an Attraction Domain for Multivariable Lur'e Systems Using Looseless Extention of the S-Procedure // Proc. Amer. Control Conf. San-Diego, 1999. P. 2395-2396.

[6] S. Boyd, L.E. Ghaoui, E. Feron, and V. Balakrishnan. Linear matrix inequalities in system and control theory. 1994. SIAM. Philadelphia.

[7] H. Khalil. Nonlinear Systems. 3rd edition. 2002. Prentice Hall.

[8] L.B. Rapoport Estimation of the domain of the exponential stability in the problem of control of wheeled robots. // Automation and Remote Control. 2006. No 9.

[9] www.javad.com